ARGET ATRP for Versatile Grafting of Cellulose Using Various Monomers

Susanne Hansson, Emma Östmark, Anna Carlmark, and Eva Malmström*

Fibre and Polymer Technology, KTH School of Chemical Science and Engineering, Royal Institute of Technology, Teknikringen 56-58, Stockholm, Sweden

ABSTRACT In recent years, cellulose-based materials have attracted significant attention. To broaden the application areas for cellulose, polymers are often grafted to/from the surface to modify its properties. This study applies ARGET (activators regenerated by electron transfer) ATRP (atom transfer radical polymerization) when straightforwardly grafting methyl methacrylate (MMA), styrene (St), and glycidyl methacrylate (GMA) from cellulose in the form of conventional filter paper in the presence of a sacrificial initiator. The free polymer, formed from the free initiator in parallel to the grafting, was characterized by ^{1}H NMR and SEC, showing that sufficient control is achieved. However, the analyses also indicated that the propagation from the surface cannot be neglected compared to the propagation of the free polymer at higher targeted molecular weights, which is an assumption often made. The grafted filter papers were evaluated with FT-IR, suggesting that the amount of polymer on the surface increased with increasing monomer conversion, which the FE-SEM micrographs of the substrates also demonstrated. Water contact angle (CA) measurements implied that covering layers of PMMA and PS were formed on the cellulose substrate, making the surface hydrophobic, in spite of low DPs. The CA of the PGMA-grafted filter papers revealed that, by utilizing either aprotic or protic solvents when washing the substrates, it was possible to either preserve or hydrolyze the epoxy groups. Independent of the solvent used, all grafted filter papers were essentially colorless after the washing procedure because of the low amount of copper required when performing ARGET ATRP. Nevertheless, surface modification of cellulose via ARGET ATRP truly facilitates the manufacturing since no thorough freeze−thaw degassing procedures are required.

KEYWORDS: ARGET ATRP • cellulose • controlled polymerization • grafting from • surface modification of cellulose • functional monomers • glycidyl methacrylate • reducing agent

INTRODUCTION

Cellulose is not only the most abundant polymer in the world; it is also an inexpensive, renewable and biodegradable organic material. Furthermore, cellulose exhibits very good mechanical properties. Cellulose-based materials are, therefore, of great interest in many applications, especially when considering the increasing environmental concern. For some applications, however, properties such as hydrophobicity and compatibility need to be improved or tailored. This is often essential to achieve better adhesion when using cellulose fibers as reinforcement in composites, especially since the matrix often is a hydrophobic polymer (1, 2). By grafting various polymers onto the cellulose surface, the hydrophobicity can be enhanced. By utilizing ring-opening polymerization (ROP) from biopolymers, it is possible to produce biocomposites (3, 4). Furthermore, new functionalities such as superhydrophobicity, stimuli-responsivity (5), liquid crystallinity (6), and antibacterial properties (7) can also be introduced to the material, exploring new application possibilities, compared to the traditional usage of cellulose as a raw material for paper, board, and construction.

A solid surface can be covalently modified by either using a "grafting to" or a "grafting from" technique. In the "grafting from" process, the polymer chains grow from initiating sites or immobilized initiators on the surface; consequently, the grafting density becomes higher compared to the "grafting to" method, where preformed polymer chains have to diffuse to the surface. Hence, in most cases, the surface-initiated polymerization technique is the preferred method (8).

To tailor the properties of cellulose, various substrates have previously been modified with controlled radical polymerization (CRP) methods (5, 9). Reversible addition−fragmentation chain transfer (RAFT) polymerization is one technique that has been employed to graft polymers from cellulose surfaces (10, 11); however, this process requires pretreatment with base prior to grafting, which may result in rearrangement of cellulose I to cellulose II. Atom transfer radical polymerization (ATRP), the most widely used CRP method, is a versatile and compatible method for a wide range of vinyl monomers and solvents, providing polymers with controlled molecular weights and low polydispersities (12−14). Grafting of cellulose via ATRP is a mild approach that does not need any pretreatment with base. In recent years, our research group has been working with surface modification of cellulose substrates via ATRP (2, 5, 15, 16).

Surface-initiated ATRP (SI-ATRP) is a suitable technique for cellulose grafting since the available hydroxyl group on the surface can easily be converted to α-bromoesters, which are known to be excellent initiators for ATRP (17). SI-ATRP can be conducted either in the presence or in the absence

© 2009 American Chemical Society

of a sacrificial initiator. From a processing point of view, it is often undesirable to form a bulk polymer in parallel to the polymer on the surface since the unbound polymer has to be removed. However, the available surface area of a solid substrate like cellulose is limited, resulting in an overall concentration of dormant species immobilized on the surface that is too low to obtain a controlled polymerization. Since ATRP relies on a dynamic equilibrium between active and dormant species, a sacrificial initiator can be utilized to adjust the concentration (8). In addition, it can also be beneficial to add a sacrificial initiator to the bulk, assuming that the bulk polymerization proceeds at the same rate as the surface polymerization. The unbound polymer can subsequently be analyzed with respect to molecular weight and polydispersity, giving an estimation of the properties of the grafted polymer, since the hypothesis proposes that their conformity is fairly good (18).

One crucial disadvantage of SI-ATRP, however, is that it requires a relatively large amount of a transition metal catalyst, often based on copper. Consequently, the grafted substrates become colored and purification is necessary to remove the catalyst complex. A large amount of catalyst, combined with its removal or recycling, increases the costs for industrial productions (19, 20). Furthermore, it can result in limitations for some applications because of environmental concerns. Another disadvantage is that the ATRP reaction has to be conducted in a completely inert atmosphere, which may further complicate the process (17).

A new approach to conduct ATRP has, therefore, been developed by Matyjazewski et al. (20) This technique is based on "activators regenerated by electron transfer" or ARGET ATRP. In ARGET ATRP, an inactive Cu(II) salt, which is added from the beginning of the polymerization, is rapidly reduced to an active Cu(I) species by a reducing agent.

The beauty of ARGET ATRP is that the amount of copper can be significantly reduced since the oxidatively stable Cu(II) complexes are constantly transformed to active Cu(I) species by the reducing agent. Consequently, only a few ppm of copper is required to mediate the polymerization (20, 21). In addition, ARGET ATRP can tolerate a large excess of the reducing agent and, as a result, the reaction can be conducted in the presence of limited amounts of air (17, 20). Surface-initiated ARGET ATRP from a silicon wafer without the need for any deoxygenation has been performed (17). To the best of our knowledge, surface modification of cellulose *via* ARGET ATRP has not yet been reported in the literature.

Ascorbic acid (AsAc) is frequently used as an environmentally friendly reducing agent. Since it is a strong reducing agent, its solubility in the reaction medium should be limited to avoid a too high concentration of radicals, which reduces the control over the polymerization. Therefore, anisole is preferred as solvent (22). It is also possible to use sodium ascorbate (NaAsc), the salt of AsAc, as a reducing agent; however, its usage in ARGET ATRP has not yet been reported. In this study, NaAsc was applied when styrene was

polymerized. A more frequently used reducing agent is tin(II) 2-ethylhexanoate ($Sn(EH)_2$) (17, 20).

Glycidyl methacrylate (GMA) is a functional monomer of commercial interest. GMA has been utilized in several applications, such as surface modification and adhesives (23). Grafting of GMA yields surfaces with pendant epoxy groups suitable for further modification as the epoxide can be reacted with carboxyl, hydroxyl, amino, and anhydride functional groups (24, 25). By grafting a functional polymer like PGMA from cellulose surfaces, the application area for cellulose-based materials could be increased. Furthermore, if the PGMA-brushes grafted from cellulose are hydrolyzed, additional hydroxyl groups becomes available on the surface, providing a higher postgrafting density (9).

This paper presents a straightforward method for grafting a cellulose substrate with a range of various monomers (methyl methacrylate (MMA), styrene (St), and glycidyl methacrylate (GMA)) using ARGET ATRP (Scheme 1). Whatman No. 1 filter paper was chosen since it is a well-characterized substrate with high cellulose content and surface area. Despite the different natures of the three monomers, the only parameters that need to be altered are the reducing agent (AsAc or NaAsc) and the temperature. Furthermore, only a short time of purging with argon is required. The main focus herein is, however, not to obtain a system with perfect control, but rather to be able to modify the surface properties of cellulose with a robust method that needs only minor adjustments for various monomers.

EXPERIMENTAL SECTION

Materials. α-Bromoisobutyryl bromide (BiB, 98%), ethyl 2-bromoisobutyrate (EBiB, 98%), 4-(dimethylamino)pyridine (DMAP, 99%), copper(II) bromide ($Cu(II)Br_2$, 99%), N,N,N',N'',N''-pentamethyldiethylenetriamine (PMDETA, 99%), and Whatman 1 filter paper were purchased from Aldrich. Sodium ascorbate (NaAsc) was purchased from Sigma. Ascorbic acid (AsAc, 99%) was purchased from Fluka. Triethylamine (TEA) was purchased from Merck. The monomers, methyl methacrylate (MMA, 99%, Aldrich), styrene (St, 99%, Fluka), and glycidyl methacrylate (GMA, 97%, Fluka), were passed through a column of neutral aluminum oxide prior to use to remove the inhibitor.
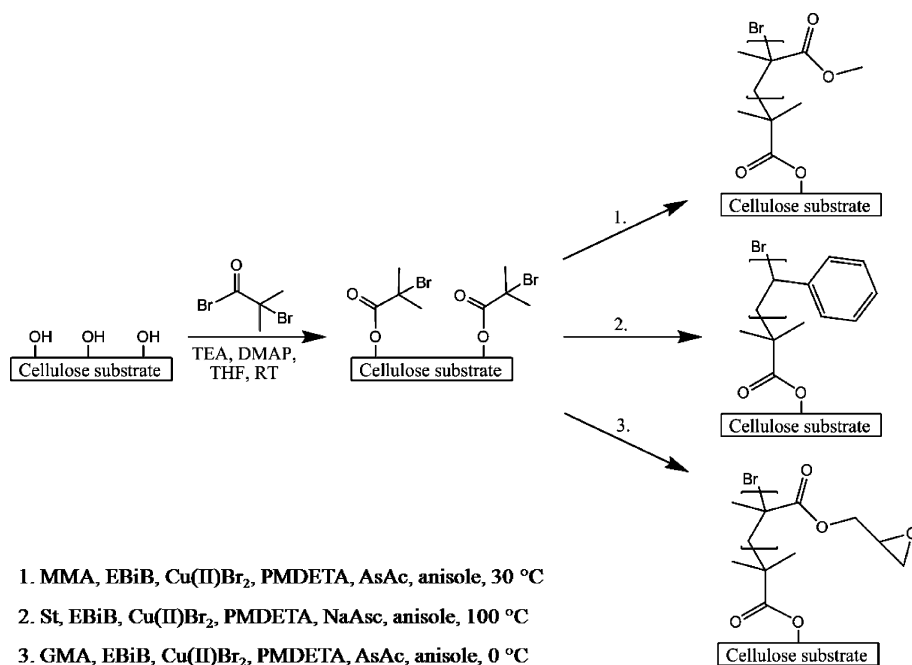
Instrumentation. ^{1}H NMR spectra were recorded on a Bruker Avance 400 MHz NMR instrument, using $CDCl_3$ as solvent. The solvent residual peak was used as internal standard.

Size exclusion chromatography (SEC) using THF (1.0 mL min^{-1}) as the mobile phase was performed at 35 °C using a Viscotek TDA model 301 equipped with two GMH$_{HR}$-M columns with TSK-gel (mixed bed, MW resolving range: 300−100 000 Da) from Tosoh Biosep, a VE 2500 GPC autosampler, a VE 1121 GPC solvent pump, and a VE 5710 GPC degasser (all from Viscotek Corp., The Netherlands). A universal calibration method was created using narrow linear polystyrene standards. Corrections for the flow rate fluctuations were made using toluene as an internal standard. Viscotek OmniSEC version 4.0 software was used to process data.

Infrared spectra were recorded on a Perkin-Elmer Spectrum 2000 FT-IR equipped with a MKII Golden Gate, single reflection ATR System (from Specac Ltd., London, U.K.). The ATR-crystal was a MKII heated Diamond 45° ATR Top Plate.

Contact angle measurements were performed at 50% RH and 23 °C and conducted on a KSV instruments CAM 200 equipped with a Basler A602f camera, using 5 μL droplets of

Scheme 1. ARGET ATRP of Various Monomers from a Cellulose Substrate

1. MMA, EBiB, Cu(II)Br$_2$, PMDETA, AsAc, anisole, 30 °C

2. St, EBiB, Cu(II)Br$_2$, PMDETA, NaAsc, anisole, 100 °C

3. GMA, EBiB, Cu(II)Br$_2$, PMDETA, AsAc, anisole, 0 °C

deionized water. The water contact angles were determined using the CAM software.

Field-emission scanning electron microscope (FE-SEM) images were recorded on a Hitachi S-4800 FE-SEM. The samples were mounted on a substrate with carbon tape and coated 3 s of a carbon coater (Cressington 108carbon/A) and subsequently 2 × 4 nm of a gold/palladium sputter coater (Cressington 208HR).

Immobilization of Initiator on Filter Paper. The procedure for immobilization of initiator on the cellulose surface was adopted from Carlmark and Malmström (15). Prior to the immobilization of the initiator, filter papers (2 × 3 cm) were washed with ethanol, acetone, and tetrahydrofuran (THF) and also ultrasonicated for 2 min in each solvent. The available hydroxyl groups on the surface were converted into ATRP initiators by immersing the filter paper in a solution containing α-bromoisobutyryl bromide (BiB) (305 mg, 1.33 mmol), TEA (148 mg, 1.46 mmol), and a catalytic amount of DMAP in THF (20 mL). The reaction was allowed to proceed for 4 h at room temperature on a shaking device. Thereafter, the filter paper was thoroughly washed in THF and ethanol, to remove residual reactants and byproduct. The filter paper was finally dried in a vacuum oven at 50 °C.

Grafting of Methyl Methacrylate from Initiator-Functionalized Filter Paper. The initiator-modified filter paper (2 × 3 cm) was immersed into a 25 mL round-bottomed flask containing anisole (10 g), MMA (10 g, 0.10 mol), EBiB (48.8 mg, 0.25 mmol; 24.4 mg, 0.13 mmol), Cu(II)Br$_2$ (5.6 mg, 25 μmol; 2.8 mg, 13 μmol), PMDETA (43.3 mg, 0.25 mmol; 21.7 mg, 0.13 mmol), and AsAc (44.0 mg, 0.25 mmol; 22.0 mg, 0.13 mmol), targeting the final DP of 400 and 800, respectively. The flask was sealed with a rubber septum and degassed with argon for 5 min, before being placed in a thermostatted oil bath at 30 °C. The kinetics was monitored by performing six parallel experiments with polymerization times between 30 min and 8 h, instead of withdrawing aliquot samples from one experiment. When the set polymerization time was reached, the reaction solution was exposed to air and diluted with DCM. The grafted filter paper was transferred to an Erlenmeyer flask, before the free polymer (formed from the sacrificial initiator) was precipitated in cold methanol and thereafter dried in a vacuum oven at 50 °C. The grafted filter paper was thoroughly

rinsed in DCM, THF, THF:water (1:1), water, methanol, and ethanol, and finally dried in a vacuum oven at 50 °C.

Grafting of Styrene from Initiator-Functionalized Filter Paper. The initiator-modified filter paper (2 × 3 cm) was immersed into a 25 mL flask containing anisole (10 g), St (10 g, 0.10 mol), EBiB (46.8 mg, 0.24 mmol; 23.4 mg, 0.12 mmol), Cu(II)Br$_2$ (5.4 mg, 24 μmol; 2.7 mg, 12 μmol), PMDETA (41.6 mg, 0.24 mmol; 20.8 mg, 0.12 mmol), and NaAsc (47.5 mg, 0.24 mmol; 23.8 mg, 0.12 mmol), targeting the final DP of 400 and 800, respectively. The same procedure as for polymerization of MMA was applied, with the exception of the usage of a higher reaction temperature of 100 °C.

Grafting of Glycidyl Methacrylate from Initiator-Functionalized Filter Paper. The initiator-modified filter paper (2 × 3 cm) was immersed into a 25 mL flask containing anisole (10 g), GMA (10 g, 70.3 mmol), EBiB (48.8 mg, 0.18 mmol), Cu(II)Br$_2$ (3.9 mg, 18 μmol), PMDETA (43.3 mg, 0.18 mmol), and AsAc (15.5 mg, 88 μmol), targeting the final DP of 400. The subsequent steps were executed similarly to the other polymerization procedures, with the exceptions that degassing and polymerization were conducted in an ice bath, and that only four experiments were performed in parallel with polymerization times between 1−4 h.

RESULTS AND DISCUSSION

ATRP provides an unprecedented possibility to grow polymer chains directly from a substrate in a controlled manner, given that there are initiating sites available on the surface. To adjust the concentration of dormant species during the surface-initiated polymerization, a sacrificial initiator can be employed. The aim of the present study is, however, not to obtain truly monodisperse grafts but to accomplish a sufficiently good control over the polymerization so that a thick enough surface layer of polymer chains is formed with preserved control over chain ends.

The grafting from cellulose surfaces via ARGET ATRP was easily conducted by immersing an initiator-functionalized filter paper in a one-pot solution of the monomer (MMA, St or GMA), anisole, EBiB, Cu(II)Br$_2$, PMDETA, and the reducing

Table 1. Experimental Conditions and Properties of Representative ARGET ATRP Experiments

entry	monomer	DP_{target}	Cu(II)[a] (ppm)	reaction time (h)	conv.[b](%)	$M_{n,theo}$[c]	$M_{n,SEC}$	M_w/M_n
1	MMA	400	250	1.5	12	5100	8100	1.09
2	MMA	400	250	4	25	10 400	10 900	1.17
3	MMA	800	125	1	7	5800	12 000	1.17
4	MMA	800	125	8	48	38 500	30 100	1.14
5	St	400	250	2	18	7500	6200	1.4
6	St	400	250	8	48	20 200	18 600	1.14
7	St	800	125	2	6	5200	7300	1.6
8	St	800	125	8	36	30 200	24 800	1.35
9	GMA	400	250	1	9	5300	10 600[d]	1.35[d]
10	GMA	400	250	4	37	21 200	17 600[d]	1.7[d]

[a] Molar ratio of Cu(II) to monomer. [b] Monomer conversion calculated from ^{1}H NMR. [c] $M_{n,theo} = DP \times MW_{monomer} \times conv. + MW_{initiator}$. [d] Value obtained from a crude sample.

agent (AsAc or NaAsc), which subsequently was purged with argon for five minutes. By varying the ratio of monomer to sacrificial initiator and assuming that the amount of initiator on the substrate is negligible, different DPs were targeted.

ARGET ATRP is a very attractive method because of the low amounts of copper required. In this study, the concentration of Cu(II) was kept relatively low (see Table 1); consequently, the grafted filter papers were essentially colorless after customary washing. Moreover, the precipitated polymer, formed from the sacrificial initiator, needed no further purification. These circumstances hold for all three investigated polymers: PMMA, PS, and PGMA.

The kinetics were monitored by analyzing the free polymer with ^{1}H NMR spectroscopy and size exclusion chromatography (SEC), also providing estimations of molecular weights and PDI values of the grafts. Since multiple experiments with the same reaction conditions were performed in parallel, the human factor must be considered when evaluating the results, due to the difficulties associated with identical reproduction of experimental conditions. Table 1 summarizes a compilation of representative experiments.

Grafting of PMMA from Cellulose. The grafting of MMA from initiator-functionalized filter paper via ARGET ATRP was conducted in anisole at 30 °C. The target DPs were 400 and 800 ([MMA]/[EBiB]/[Cu(II)Br$_2$]/[PMDETA]/[AsAc] = DP_{target}:1:0.1:1:1). Six parallel experiments were performed and run for different reaction times, ranging from between 30 min to 8 h (Table 1, entries 1−4).

The free polymer formed simultaneously to the grafting was analyzed by ^{1}H NMR and SEC. The kinetic plot, which is based on the conversion determined from ^{1}H NMR, is shown in Figure 1 (Table 1, entries 1−4). The reaction is first-order with respect to monomer conversion for both target DPs. The molecular weights and the polydispersities of the crude samples of PMMA (DP_{target} 800) as a function of conversion are illustrated in Figure 2, whereas Table 1, entries 1−4, presents the molecular weights and PDI values of the precipitated polymers. Figure 2 shows that at low monomer conversions the molecular weight received from SEC is higher than the theoretical value obtained from ^{1}H NMR, suggesting limited initiator efficiency. The incomplete
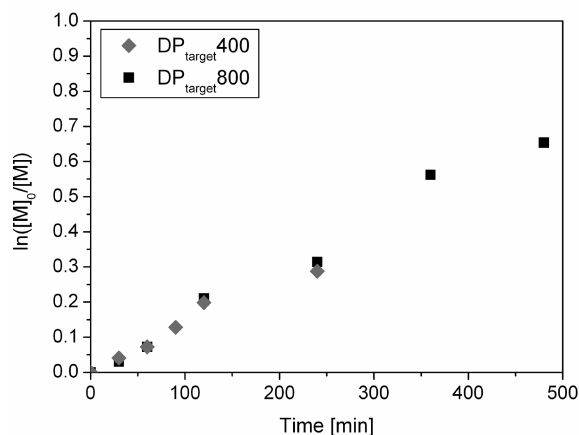

FIGURE 1. Kinetic plot for ARGET ATRP of PMMA. Experimental conditions: ◆ [MMA]/[EBiB]/[Cu(II)Br$_2$]/[PMDETA]/[AsAc] = 400:1:0.1:1:1), ■ [MMA]/[EBiB]/[Cu(II)Br$_2$]/[PMDETA]/[AsAc] = 800:1:0.1:1:1), [MMA]$_0$ = 9.35 M, T = 30 °C, in anisole (50 wt %).
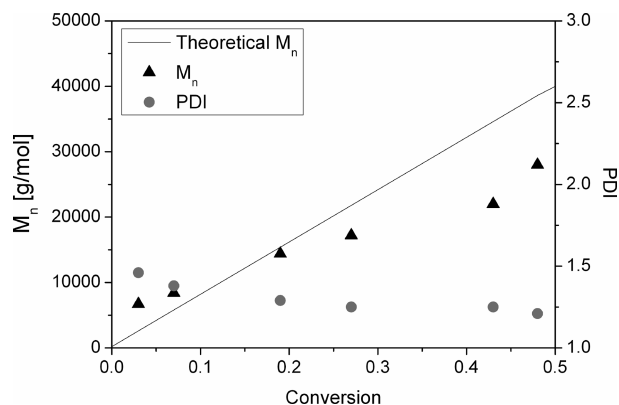

FIGURE 2. Molecular weight and PDI of PMMA as a function of monomer conversion. The continuous line represents the theoretical values that were calculated from the monomer conversion determined by ^{1}H NMR. Experimental conditions: [MMA]/[EBiB]/[Cu(II)Br$_2$]/[PMDETA]/[AcAs] = 800:1:0.1:1:1; [MMA]$_0$ = 9.35 M, T = 30 °C, in anisole (50 wt %).

initiation of EBiB is probably caused by its activation rate, which is approximately eight times smaller compared to that when a monomer is added to a growing PMMA chain (21). Consequently, the initiation is not as fast as desired for an ATRP reaction. At higher monomer conversions, on the
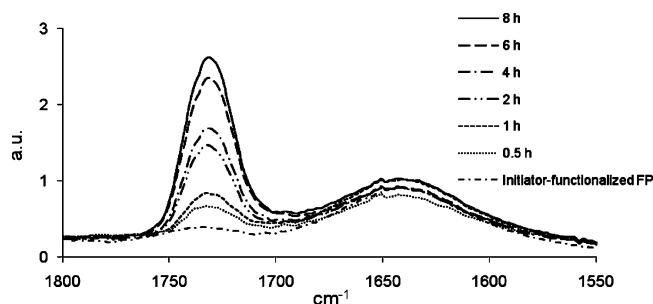
FIGURE 3. FT-IR spectra of PMMA-grafted cellulose at different reaction times (DP$_{target}$ 800) showing the carbonyl region.

other hand, the molecular weight is lower than the theoretical value, which probably is because the surface propagation contributes to the consumption of monomers to a larger extent than believed, indicating that the surface area cannot be neglected at higher monomer conversions. This especially holds for higher target DPs, since fewer propagating chains are then present. Additionally, more chains may have been initiated as the reaction proceeds and, consequently, more monomers would be consumed. Limited initiator efficiency could, therefore, also lead to poor reproducibility between the parallel experiments. However, a certain deviation between the theoretical molecular weight and the molecular weight obtain from the SEC is anticipated since the SEC is calibrated using PS standards. Nevertheless, the molecular weights of the formed polymers are rather close to theoretical values. Figure 2 also demonstrates that the PDI decreases with increasing monomer conversion.

To confirm successful grafting, all grafted substrates were characterized with FT-IR spectroscopy, water contact angle (CA) measurements, and scanning electron microscopy (FE-SEM). Figure 3 shows the FT-IR spectra of the PMMA-grafted surfaces at different reaction times (DP$_{target}$ 800). As can be seen, the carbonyl content (peak at 1730 cm^{-1}) increases successively with reaction time, suggesting that it is possible to tailor the amount of polymer on the surface.

The surface coverage of the grafted filter papers was evaluated by CA measurements. The CA is affected by the chemical composition of the surface and also the surface roughness. The inherent roughness of filter papers renders it difficult to determine absolute values; hence, the contact angles are only approximate. The unmodified filter paper absorbs the water droplet immediately, whereas the PMMA-grafted filter paper with a relatively low DP (Table 1, entry 3) displayed a stable CA of 109° ± 3°. The CA of the cellulose substrate grafted with a higher DP (Table 1, entry 4) was 112° ± 2°, suggesting that there is no significant divergence between the two samples. In other words, the CA of cellulose is largely increased via grafting of PMMA but is not directly affected by the length of the grafts, confirming that the hydrophilic character of cellulose can easily be modified.

Figure 4 depicts FE-SEM micrographs of unmodified cellulose (a) and PMMA-grafted cellulose after one (b) and eight hours (c) with a target DP of 800. The fine surface structure of cellulose, which is evident in Figure 4a, cannot be as easily distinguished in Figure 4b and c. This is because

of the smoothing effect that the grafted polymers have on the surface, making the structure less rough. Nevertheless, Figure 4 also establishes that the fibril structure of cellulose is preserved. By comparing Figure 4b and c, an apparent difference in the amount of polymer present on the surface can be perceived, corroborating the results from FT-IR spectroscopy.

Grafting of PS from Cellulose. Styrene was grafted from initiator-functionalized filter paper in anisole at 100 °C. The same polymerization procedure as for PMMA was used; however, instead of AsAc as a reducing agent, NaAsc was employed to obtain a sufficiently soluble reaction mixture. ARGET ATRP of styrene has previously been performed with AsAc as a reducing agent; however, tris(2-(dimethylamino)ethyl)amine (Me$_6$TREN) was utilized as a ligand (22).

The kinetic plot of PS, formed in parallel to the grafting, is outlined in Figure 5 (Table 1, entries 5−8). As can be seen, data for the two polymerizations with DP$_{target}$ 400 and DP$_{target}$ 800 does not overlap. This discrepancy may be the result of the presence of fewer propagating chains in the solution at a higher target DP; consequently, the propagation from the surface has a large impact on the monomer consumption. Therefore, the amount of initiating sites on the surface cannot be neglected compared to the amount of sacrificial initiator when aiming for higher molecular weights, which the results from the PMMA grafting also indicated. Figure 5 also shows that there is an induction period where the Cu(II) species are proposed to be reduced to Cu(I) complexes (26). This phenomenon is, however, not observed for PMMA. This can be explained by the fact that NaAsc is a weaker reducing agent than AsAc. Another reason may be that EBiB is a more suitable initiator for MMA than for styrene, due to better structural resemblance (27). However, the slope of the two curves in Figure 5 appears to be almost the same, indicating that the apparent rate constant is similar in the two experiments. The polymerization seems to be a first-order reaction.

The molecular weights and the PDI values of the crude samples of PS are plotted in Figure 6 (DP$_{target}$ 800), suggesting that there is only a minor difference between the molecular weights attained from the SEC and the theoretical values. The same behavior as for PMMA is shown, with slightly higher molecular weights compared to the theoretical values at lower monomer conversions and the opposite at higher conversions. However, these molecular weights correspond better to the theoretical values than for the PMMA samples, since the SEC is calibrated using PS standards. Table 1, entry 5−8, gives the molecular weights and PDI values of the precipitated polymers.

FT-IR spectra of PS-grafted surfaces at different reaction times (DP$_{target}$ 800) are depicted in Figure 7 and show a similar trend as for the PMMA-grafted surfaces. The peak around 700 cm^{-1}, corresponding to the phenyl ring in styrene (28), increases with increasing monomer conversion. However, the signal from the aromatic structure is not as strong as that of the carbonyl group since its extinction coefficient is much smaller. There are, therefore, no obvious differences at lower monomer conversions.
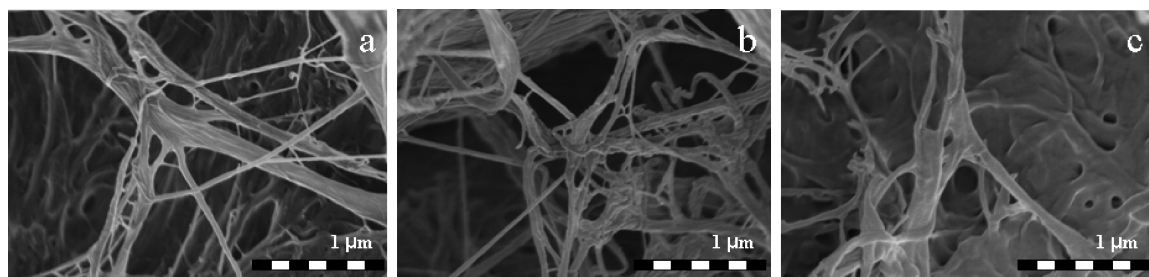
FIGURE 4. FE-SEM images of unmodified cellulose (a) and PMMA-grafted cellulose with DP_{target} 800 for one hour (b) and eight hours (c) with 30 000× magnification.
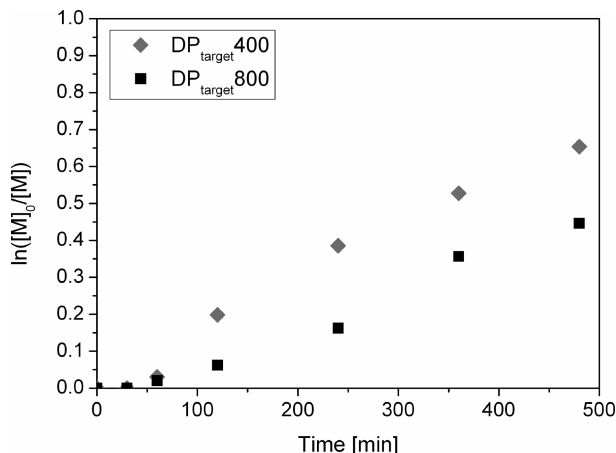

FIGURE 5. Kinetic plot for ARGET ATRP of styrene. Experimental conditions: ◆ [St]/[EBiB]/[Cu(II)Br$_2$]/[PMDETA]/[NaAsc] = 400:1:0.1: 1:1), ■ [St]/[EBiB]/[Cu(II)Br$_2$]/[PMDETA]/[NaAsc] = 800:1:0.1:1:1), [St]$_0$ = 8.73 M, T = 100 °C, in anisole (50 wt %).
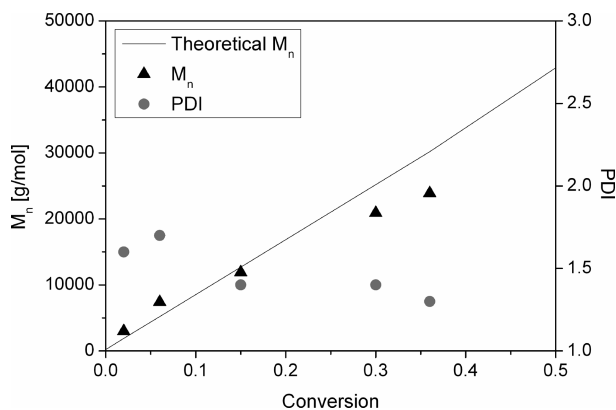

FIGURE 6. Molecular weight and PDI of PS as a function of monomer conversion. The continuous line represents the theoretical values that were calculated from the monomer conversion determined by ^{1}H NMR. Experimental conditions: [St]/[EBiB]/[Cu(II)Br$_2$]/[PMDETA]/[NaAsc] = 800:1:0.1:1:1. [St]$_0$ = 8.73 M, T = 100 °C, in anisole (50 wt %).

The CA measurements of the PS-grafted filter papers also showed increased hydrophobicity. The shorter grafts (Table 1, entry 7) displayed a slightly higher CA than the substrate with longer PS-grafts (Table 1, entry 8); 137° ± 1° compared to 132° ± 3°. The very small decrease of the CA may be due to the fact that longer polymer chains smooth the surface more; in other words, the reduced surface roughness leads to a lower CA. The difference, however, is practically insignificant, since the contact angles are only approximate.
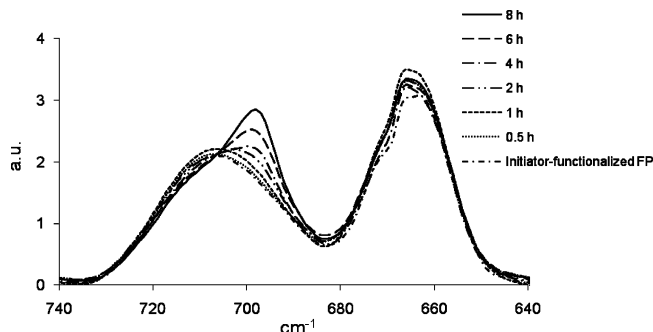

FIGURE 7. FT-IR spectra of PS-grafted cellulose at different reaction times (DP_{target} 800) showing the aromatic region.

Nevertheless, the results propose that the surface properties are altered already at very low monomer conversion.

Figure 8 displays the FE-SEM images of unmodified cellulose (a) and PS-grafted cellulose after two (b) and eight hours (c), DP_{target} 800. In agreement with the FE-SEM images of PMMA-grafted cellulose, there is a difference in the surface structure between the unmodified cellulose and the two grafted surfaces. In particular, Figure 4c displays a smoother surface structure, verifying the result from the CA measurements.

Grafting of PGMA from Cellulose. GMA is a very interesting monomer since it has both epoxide and methacrylate functionalities, making it possible to utilize ARGET ATRP to yield polymers with pendant epoxide groups. It is, however, also a challenging monomer due to the highly reactive oxirane ring, which is prone to undergo ring-opening, with gelation as a consequence (29). The grafting from initiator-functionalized filter paper had to be performed at 0 °C (in anisole); otherwise, a gel was formed. In order to avoid gelation due to ring-opening, the monomer conversions should not exceed approximately 40 %; above that the conversion began to decrease, suggesting gelation. This limit has also been reported by Jonsson et al. (30), who propose to utilize a very low copper concentration, below 100 ppm, to suppress gel formation. Additionally, the amount of the reducing agent had to be decreased to attain an acceptable polymerization rate. Another attempt to reduce the reaction rate was to utilize NaAsc instead of AsAc, since NaAsc is a weaker reducing agent. However, this led to gelation at even lower conversion than when AsAc was applied, suggesting a higher sensitivity toward basic conditions than acidic. As an alternative, Sn(EH)$_2$ may circumvent the gelation more successfully, since this reducing agent is neither acidic nor basic.
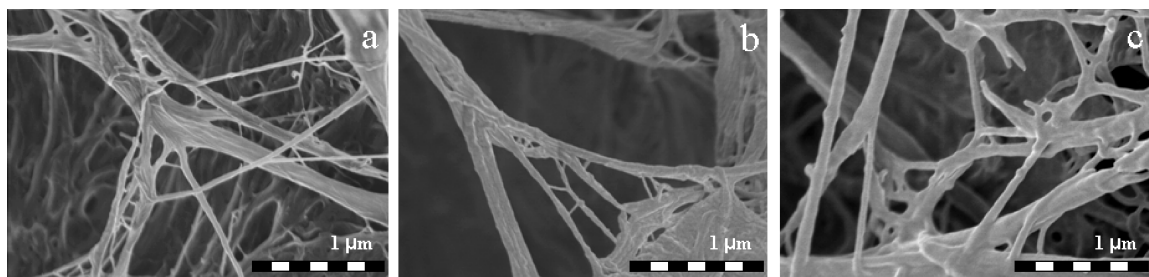
FIGURE 8. FE-SEM images of unmodified cellulose (a) and PS-grafted cellulose with a DP_{target} 800 after two hours (b) and eight hours (c) with $30\,000\times$ magnification.
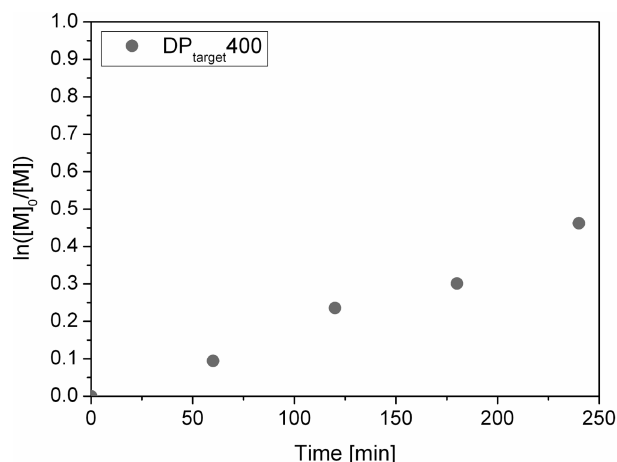

FIGURE 9. Kinetic plot for ARGET ATRP of GMA. Experimental conditions: $[GMA]/[EBiB]/[Cu(II)Br_2]/[PMDETA]/[AsAc] = 400:1:0.1:1:0.5$; $[GMA]_0 = 7.56$ M, $T = 0$ °C, in anisole (50 wt %).
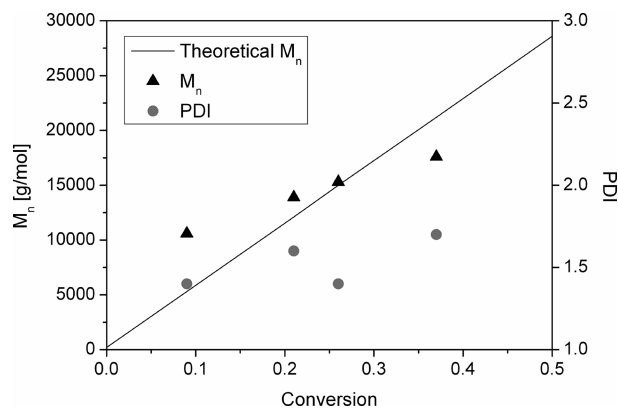

FIGURE 10. Molecular weight and PDI of PGMA as a function of monomer conversion. The continuous line represents the theoretical values that were calculated from the monomer conversion determined by ^{1}H NMR. Experimental conditions: $[GMA]/[EBiB]/[Cu(II)Br_2]/[PMDETA]/[AsAc] = 400:1:0.1:1:0.5$; $[GMA]_0 = 7.56$ M, $T = 0$ °C, in anisole (50 wt %).

The target DP was 400 ($[GMA]/[EBiB]/[Cu(II)Br_2]/[PMDETA]/[AsAc] = 400:1:0.1:1:0.5$), and four parallel experiments were conducted between one and four hours (Table 1, entries 9 and 10).

Even though several attempts were made to slow down the reaction, it was difficult to obtain a system with satisfactory control. However, the kinetic plot of the free-formed polymer (Figure 9) shows a first-order reaction. Figure 10 presents the molecular weights and the PDI values as a function of monomer conversion (Table 1, entries 9 and 10), showing the same trend as for PMMA and PS. All data are
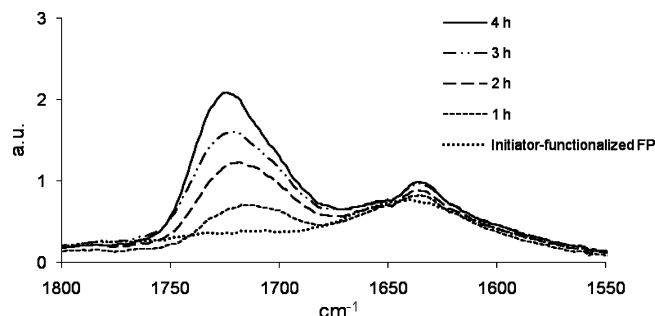

FIGURE 11. FT-IR spectra of PGMA-grafted cellulose at different reaction times (DP_{target} 400) showing the carbonyl region.

based on crude samples since the precipitated polymers became insoluble after being stored for a while, which probably was caused by the cross-linking of the epoxy groups. Furthermore, when the samples were dried in a vacuum oven at 50 °C, the process may have been further accelerated.

Figure 11 displays the FT-IR spectra of the PGMA-grafted surfaces at different reaction times, showing the same regular increase of the carbonyl content as the PMMA-grafted surfaces.

CA was also performed on the PGMA-grafted filter papers with shorter and longer DPs (Table 1, entries 9 and 10). The filter paper with the longer grafts (i.e., more polymer) absorbed the entire water droplet, whereas it was only initially absorbed by the cellulose surface with the shorter grafts. These results indicate that some or most of the epoxy groups on the surface have been opened, which probably depends on the thorough washing procedure that was performed in a variety of protic solvents. To investigate this, PGMA was once more grafted from an initiator-functionalized filter paper as previously described. The substrate was subsequently cut in two; one piece was washed with protic solvents (tetrahydrofuran:water, water, methanol, and ethanol), and the other by utilizing aprotic solvents (dichloromethane, acetone, tetrahydrofuran, and diethyl ether). Regardless of the solvent employed, both pieces were essentially colorless because of the low amount of copper in the system. Furthermore, CA measurements showed that when only aprotic solvents were used, the water droplet was stable over a long time, while the other piece absorbed the droplet at once. These results suggest that the washing process greatly influences the PGMA-grafted filter papers. Nevertheless, the opening of the epoxides introduces more accessible hydroxyl groups on the surface without the need
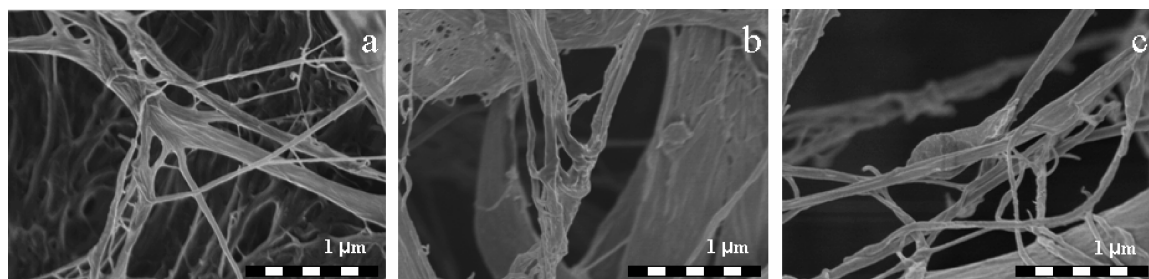
FIGURE 12. FE-SEM images of unmodified cellulose (a) and PGMA-grafted cellulose with DP_{target} 400 after one hour (b) and after four hours (c) with $30\,000\times$ magnification.

for any further hydrolysis step, making it easier to postfunctionalize the surface.

The FE-SEM images of unmodified cellulose (a) and PGMA-grafted cellulose after one (b) and four hours (c) with a target DP of 400, presented in Figure 12, suggest a smoothing tendency upon grafting, as for the other polymers. In other words, the surface coating of cellulose is more evident at longer reaction times, verifying that the DP of the grafted polymers can be tailored.

CONCLUSIONS

It has been demonstrated that ARGET ATRP is a very suitable method for surface modification of a cellulose substrate. Only minor adjustments to the reaction conditions had to be performed in between the polymerizations of three rather different monomers: MMA, St and GMA. Different theoretical DPs were targeted by controlling the ratio of monomer to added sacrificial initiator, assuming that the amount of initiator covalently bound to the surface was negligible. However, it was found that at higher target DP, the propagation from the surface can no longer be neglected compared to the propagation in the solution.

The kinetic study of the polymer simultaneously formed in the solution showed a first-order behavior with respect to monomer conversion for all three polymers. However, for PS there was a distinct induction period at the beginning of the reaction where the Cu(II) species are transformed to Cu(I) species. This effect was not observed for PMMA or PGMA, which may be explained by the fact that NaAsc was applied for PS instead of the stronger reducing agent AsAc, which was utilized for PMMA and PGMA. It may also be due to the fact that EBiB is a more appropriate initiator for MMA and GMA than for St, due to better structural resemblance.

By analyzing the grafted filter papers with FT-IR it could be concluded that the amount of polymer on the surface increased with increasing monomer conversion, which also the FE-SEM micrographs of the substrates verified. CA measurements suggested that the contact angles of the PMMA-grafted and PS-grafted filter papers were not significantly affected by the amount of polymer covering the surface. However, the grafting clearly showed that even a small amount of polymer greatly enhances the hydrophobicity of cellulose. The CA of PGMA-grafted filter papers revealed that the washing procedure has an impact on the epoxy groups. Protic solvents tend to open some of the epoxides and thereby introduce more hydroxyl groups to the surface. Aprotic solvents, however, seem to preserve the epoxy functionality of PGMA.

By modification of cellulose surfaces, the application area for cellulose-based materials could be increased, particularly if a functional polymer like PGMA is used. Furthermore, owing to the significantly reduced amount of copper required when applying ARGET ATRP, the cellulose substrates were basically colorless after washing. This reduction of the transition metal catalyst is not only environmentally beneficial but also advantageous from an economic point of view.

REFERENCES AND NOTES

(1) Gandini, A. *Macromolecules* **2008**, *41*, 9491–9504.
(2) Lindqvist, J.; Malmström, E. *J. Appl. Polym. Sci.* **2006**, *100*, 4155–4162.
(3) Lönnberg, H.; Zhou, Q.; Brumer, H., 3rd; Teeri Tuula, T.; Malmström, E.; Hult, A. *Biomacromolecules* **2006**, *7*, 2178–85.
(4) Habibi, Y.; Goffin, A.-L.; Schiltz, N.; Duquesne, E.; Dubois, P.; Dufresne, A. *J. Mater. Chem.* **2008**, *18*, 5002–5010.
(5) Lindqvist, J.; Nyström, D.; Östmark, E.; Antoni, P.; Carlmark, A.; Johansson, M.; Hult, A.; Malmström, E. *Biomacromolecules* **2008**, *9*, 2139–2145.
(6) Westlund, R.; Carlmark, A.; Hult, A.; Malmström, E.; Saez, I. M. *Soft Matter* **2007**, *3*, 866–871.
(7) Lee Sang, B.; Koepsel Richard, R.; Morley Scott, W.; Matyjaszewski, K.; Sun, Y.; Russell Alan, J. *Biomacromolecules* **2004**, *5*, 877–82.
(8) Fukuda, T.; Tsujii, Y.; Ohno, K. *Macromol. Eng.* **2007**, *2*, 1137–1178.
(9) Nyström, D.; Lindqvist, J.; Östmark, E.; Hult, A.; Malmström, E. *Chem. Commun.* **2006**, 3594–3596.
(10) Barsbay, M.; Gueven, O.; Stenzel, M. H.; Davis, T. P.; Barner-Kowollik, C.; Barner, L. *Macromolecules* **2007**, *40*, 7140–7147.
(11) Roy, D.; Guthrie, J. T.; Perrier, S. *Macromolecules* **2005**, *38*, 10363–10372.
(12) Kato, M.; Kamigaito, M.; Sawamoto, M.; Higashimura, T. *Macromolecules* **1995**, *28*, 1721–3.
(13) Wang, J.-S.; Matyjaszewski, K. *Macromolecules* **1995**, *28*, 7901–10.
(14) Wang, J.-S.; Matyjaszewski, K. *J. Am. Chem. Soc.* **1995**, *117*, 5614–15.
(15) Carlmark, A.; Malmström, E. *J. Am. Chem. Soc.* **2002**, *124*, 900–1.
(16) Carlmark, A.; Malmström, E. E. *Biomacromolecules* **2003**, *4*, 1740–1745.
(17) Matyjaszewski, K.; Dong, H.; Jakubowski, W.; Pietrasik, J.; Kusumo, A. *Langmuir* **2007**, *23*, 4528–4531.
(18) von Werne, T.; Patten, T. E. *J. Am. Chem. Soc.* **2001**, *123*, 7497–7505.
(19) Chan, N.; Cunningham, M. F.; Hutchinson, R. A. *Macromol. Chem. Phys.* **2008**, *209*, 1797–1805.

(20) Jakubowski, W.; Min, K.; Matyjaszewski, K. *Macromolecules* **2006**, *39*, 39–45.

(21) Li, W.; Gao, H.; Matyjaszewski, K. *Macromolecules* **2009**, *42*, 927–932.

(22) Min, K.; Gao, H.; Matyjaszewski, K. *Macromolecules* **2007**, *40*, 1789–1791.

(23) Jang, J.; Bae, J.; Ko, S. *J. Polym. Sci., Part A: Polym. Chem.* **2005**, *43*, 2258–2265.

(24) Edmondson, S.; Huck, W. T. S. *J. Mater. Chem.* **2004**, *14*, 730–734.

(25) Liu, Y.; Klep, V.; Zdyrko, B.; Luzinov, I. *Langmuir* **2004**, *20*, 6710–6718.

(26) Dong, H.; Matyjaszewski, K. *Macromolecules* **2008**, *41*, 6868–6870.

(27) Matyjaszewski, K.; Xia, J. *Chem. Rev.* **2001**, *101*, 2921–2990.

(28) Socrates, G., *Infrared and Raman Characteristic Group Frequencies*, 3rd ed.; John Wiley and Sons, LTD: Chichester, U.K., 2001; pp 157–162.

(29) Safa, K. D.; Nasirtabrizi, M. H. *Polym. Bull.* **2006**, *57*, 293–304.

(30) Jonsson, M.; Nyström, D.; Nordin, O.; Malmström, E. *Eur. Polym. J.* **2009**, *45*, 2374–2382.

ARTICLE